# LS-DYNA*® Analysis of a Full-Scale Helicopter Crash Test

Martin S. Annett
*Structural Dynamics Branch*
*NASA Langley Research Center*
*Hampton, VA 23681*

## Abstract

*A full-scale crash test of an MD-500 helicopter was conducted in December 2009 at NASA Langley's Landing and Impact Research facility (LandIR). The MD-500 helicopter was fitted with a composite honeycomb Deployable Energy Absorber (DEA) and tested under vertical and horizontal impact velocities of 26 ft/sec and 40 ft/sec, respectively. The objectives of the test were to evaluate the performance of the DEA concept under realistic crash conditions and to generate test data for validation of a system integrated LS-DYNA® finite element model. In preparation for the full-scale crash test, a series of sub-scale and MD-500 mass simulator tests was conducted to evaluate the impact performances of various components, including a new crush tube and the DEA blocks. Parameters defined within the system integrated finite element model were determined from these tests. The objective of this paper is to summarize the finite element models developed and analyses performed, beginning with pre-test and continuing through post test validation.*

## Introduction

The NASA Subsonic Rotary Wing (SRW) Project is sponsoring fundamental research associated with improvements in rotorcraft crashworthiness [1]. A task to develop and validate a system integrated rotorcraft LS-DYNA® finite element model (FEM) was established within this framework. The energy absorption mechanisms of rotorcraft are characterized by thin walled nonlinear deformation, contact loading, and material response. The inclusion of all components in a single comprehensive computational model allows for interactions that might be neglected when analyzing systems using separate models. Modeling detailed representations of the frame, seats, restraints, and occupants into a single FEM is now common practice within the automotive crashworthiness community [2,3]. Efforts to conduct integrated simulations have progressed along with advances in computing power.

This paper will focus on the development of the system integrated FEM of an MD-500 helicopter outfitted with deployable energy absorbers (DEA). Data from component tests, mass simulator tests, and the culminating full-scale crash test are utilized throughout the development process. This hierarchical approach expanded confidence and mitigated uncertainties in component representation within the FEM.

## Full-Scale Test Article Description

The full-scale crash test of an MD-500 helicopter was conducted at the NASA Langley Research Center (LaRC) Landing and Impact Research facility (LandIR). The LandIR facility is a 240 ft

* *The use of commercial product names in the report is for accurate reporting and does not constitute an official endorsement, either expressed or implied, of such products or manufacturers by the National Aeronautics and Space Administration.*

tall gantry structure with swing cables attached at one end and a movable pullback platform positioned on the opposite end. Two pullback cables raise the test article to a prescribed height. Upon pyrotechnic release of the pullback cable, the test article swings along two pairs of swing cables attached to the test article. The two pairs of swing cables are equally spaced to form a parallelogram. This configuration controls pitch, roll and yaw rate during the swing. The swing cables are pyrotechnically severed prior to impact.

The test article used for the full-scale crash test includes an MD-500 helicopter fuselage and skid gear. The airframe was provided by the US Army's Mission Enhanced Little Bird (MELB) program. A photograph of the test article is shown in Figure 1. The weight of the test article is equivalent to the MD-500 maximum gross weight of 3,000 lb. The empty weight is approximately 500 lb and occupants and seat weights total 800 lb. The remainder is ballast weight representing the tail section, fuel, rotor, transmission, and engine. The weight and balance information was provided by MELB.

**Figure 1. MD-500 Test Article**

Two crew and two passenger Anthropomorphic Test Devices (ATD) are positioned in standard non-energy absorbing military seats. The crew ATDs are restrained with four point harnesses and the passenger ATDs are restrained with three-point harnesses. The pilot is a 50th percentile HYBRID III male. The co-pilot and one passenger are 50th percentile HYBRID II males. The HYBRID III ATD is modified to include a straight lumbar spine, and is similar to the lumbar spine of a HYBRID II ATD. The straight lumbar spine is used for aviation seat certification and enforces proper spinal loading for vertical impact. The second passenger is a biofidelic torso attached to a HYBRID III pelvis and legs. The biofidelic torso is the 50th percentile Human Surrogate Torso Model (HSTM50). The HSTM50 has been developed by The Johns Hopkins University Applied Physics Laboratory and contains detailed representations of organs, skeletal structure and soft tissue [4].

The DEA is a Kevlar-129 fabric/epoxy design that consists of multiple hexagonal cells [5-7]. The DEA design is illustrated in Figure 2. The cell wall flat facet width is one inch. Cell wall heights vary from 16 to 20 inches. Two DEA's blocks, spanning the fuselage belly surface, were

secured to the fuselage outer skin with parachute cord. The cord was restrained to the fuselage with two aluminum rails mounted below the door openings.

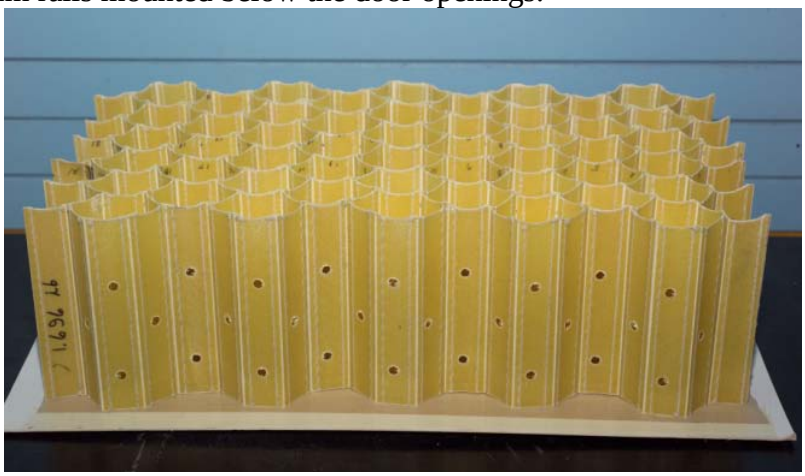

**Figure 2. DEA Design**

Vertical crush tubes were designed and fabricated which allow the skid gear to properly swing out on impact without being overloaded. The tubes are aluminum overwrapped with graphite epoxy and absorb energy through inversion drawing. Rod ends are attached at either end of the tube to impose purely axial loads through the strut length. A summary of the tube design is provided in [8]. The crush tube is shown in Figure 3.

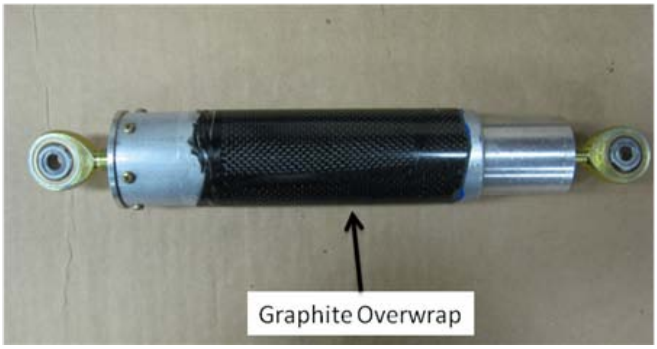


**Figure 3. Crush tube**

## MD-500 Model Development

The DEA cell walls were represented with shell elements and isotropic elastic-plastic material properties. The compaction of the DEA is directly replicated as the cell walls plastically hinge and fold [9]. The nonlinearities in the shell based option are characterized by both geometric and constitutive modeling. Convergence studies revealed that the maximum acceptable element length was approximately ⅓ inch. For the dimensions of the DEA, that corresponds to hundreds of thousands of elements per DEA component. The typical mesh refinement of a shell based DEA model is illustrated in Figure 4. The material model is *MAT_024 with a Young's Modulus of 340 ksi and initial yield stress of 7,500 psi. The yield stress versus plastic strain curve is plotted in Figure 5.

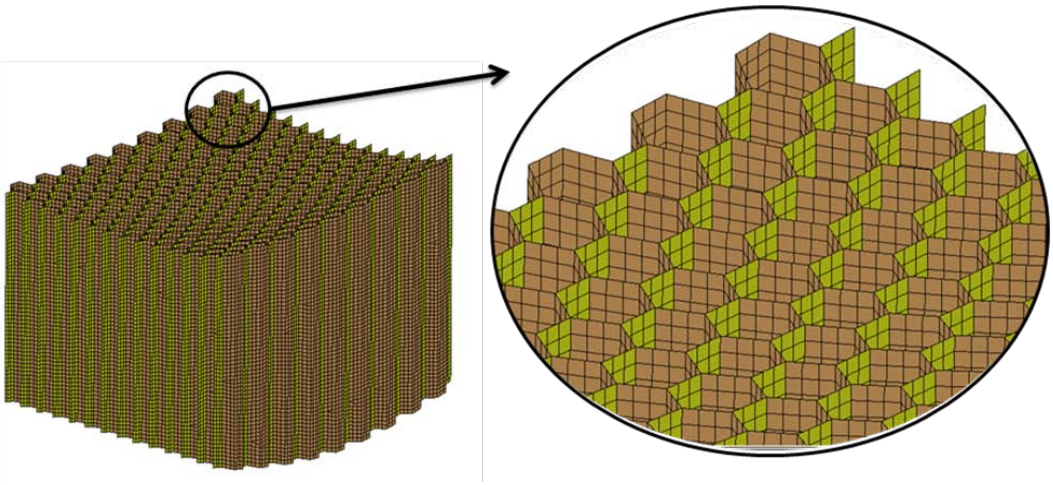

**Figure 4. Shell based DEA FEM**

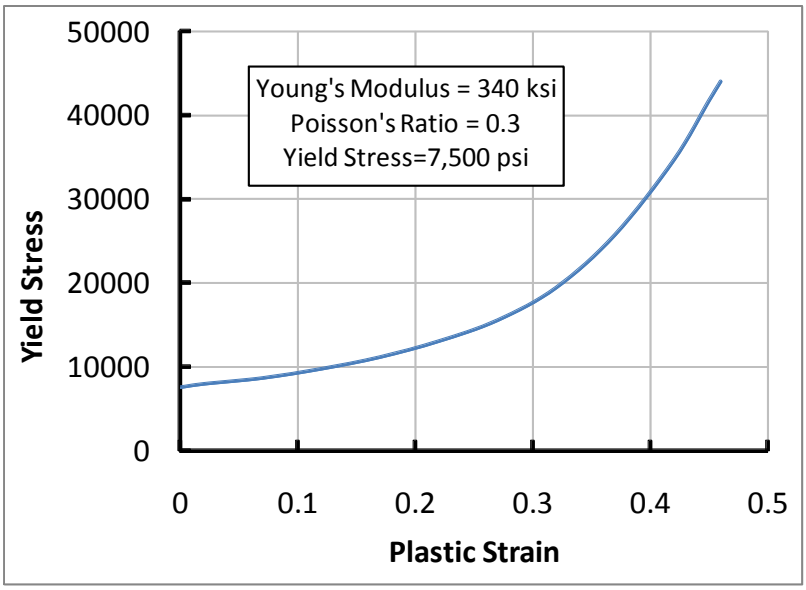


**Figure 5. DEA Yield Stress versus Plastic Strain**

The crush tubes were represented by truss elements (*SECTION_BEAM, ELFORM 3) that only transmit axial loads. The material property is *MAT_003 aluminum. The yield curve was based on the crush strength versus stroke curve from dynamic impact tests. The dynamic test setup and characteristic load time history are shown in Figure 6 [8]. A yield stress was defined equivalent to the dynamic crush load of 2,300 lb. A nearly perfectly plastic behavior is assumed upon attaining the crush load.

The skid gear is composed primarily of shell elements, with a *MAT_003 material property to represent the high strength aluminum 7075-T73 die forgings. The total weight of the skid gear is 80 lb. The finite element model of the skid gear and struts is shown in Figure 7.

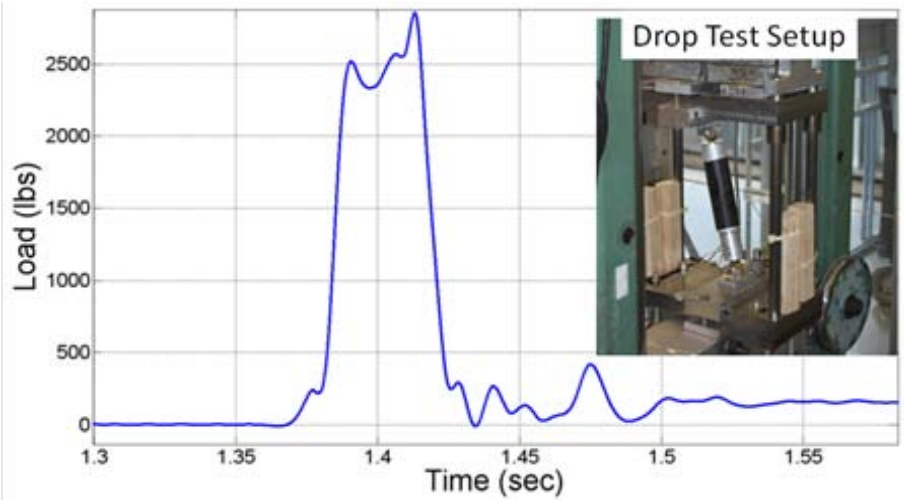


**Figure 6. Crush tube Dynamic Testing**

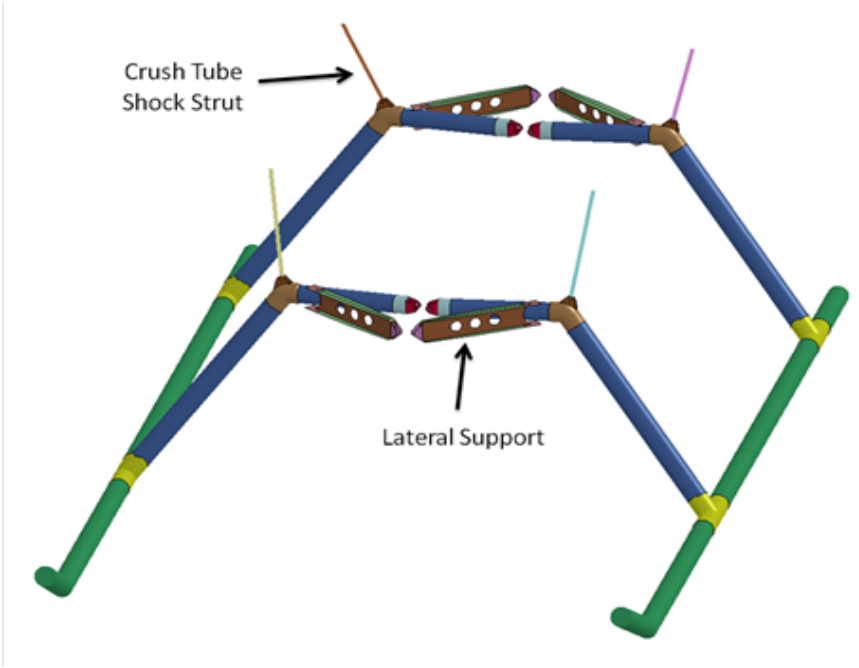


**Figure 7. Skid Gear FEM**

The performances of the skid gear, crush tubes, and the DEA were verified by conducting two crash tests of an MD-500 mass simulator. The simulator is a 2,500-lb. thick aluminum plate attached to the skid gear with stainless steel brackets and lateral supports. The mass simulator was instrumented with a triaxial accelerometer at the center of gravity (CG) and uniaxial strain gages on the vertical tubes of the skid gear. The first mass simulator test was conducted prior to DEA fabrication with polystyrene foam, and intended to primarily verify test procedures and setup.

The second mass simulator swing test was conducted at the full-scale vertical and horizontal impact velocities of 26 ft/sec and 40 ft/sec, respectively. Two DEA's, approximately 14 inches in height, were secured to the underside of the flat plate with parachute cord. Based on results

from parametric studies of the DEA [9,10], the orientation of the DEA segments was set at 20 degrees from vertical. The test article and corresponding FEM are shown in Figure 8. The pitch, roll, and yaw angles were equal to 0, 1.5, and 1.6 degrees, respectively.

The concrete surface was represented with *RIGIDWALL_PLANAR. The skid gear, lateral supports and brackets were connected with *CONSTRAINED_JOINT_REVOLUTE. The DEA's were fixed to the underside of the plate surface using *CONTACT_..._TIEBREAK. *CONTACT_AUTOMATIC_SINGLE_SURFACE was specified for the DEA for the interaction between folded and crushed shell elements.

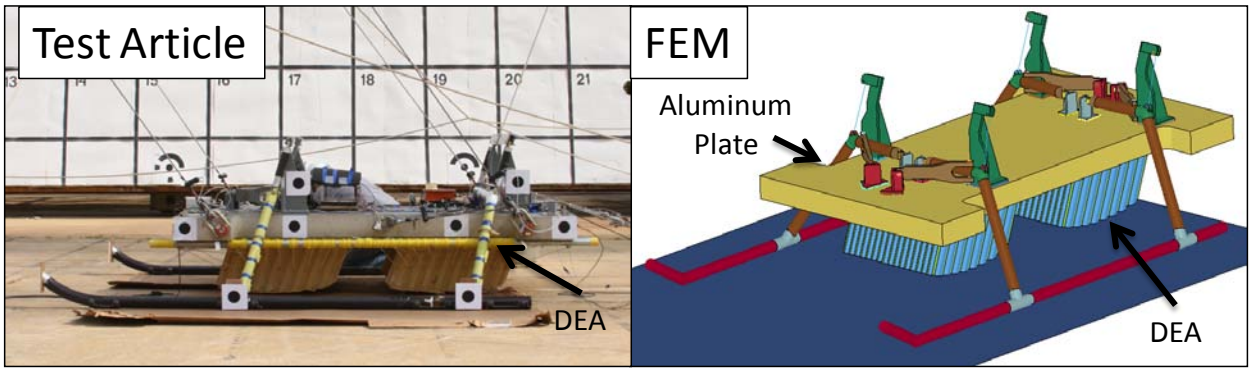


**Figure 8. MD 500 Mass Simulator with DEA**

The vertical and horizontal acceleration responses are plotted against the analysis results in Figure 9. The acceleration results were filtered with a Butterworth 50 Hz low pass filter. The pulse shapes and magnitudes for the vertical acceleration were comparable. Results from slow-rate friction drag tests performed on representative DEA sections indicated a friction coefficient of 0.5. Based on the measured horizontal accelerations, the friction coefficient of 0.5 specified in the *RIGIDWALL card was too conservative. The friction coefficient was reduced to 0.3 for all subsequent simulations with the DEA.

Test and analysis axial strains for the right forward vertical leg of the skid gear are shown in Figure 10. The vertical members are highly loaded upon impact and exhibit a tension/compression bending response. The strains do not exceed the yield allowable of the aluminum and no plastic deformation was observed from the post-test examination of the skid gear. Strain results compare well between test and analysis. The modeling approach for the skid gear and the crush tubes was deemed adequate based on the high level of correlation obtained.

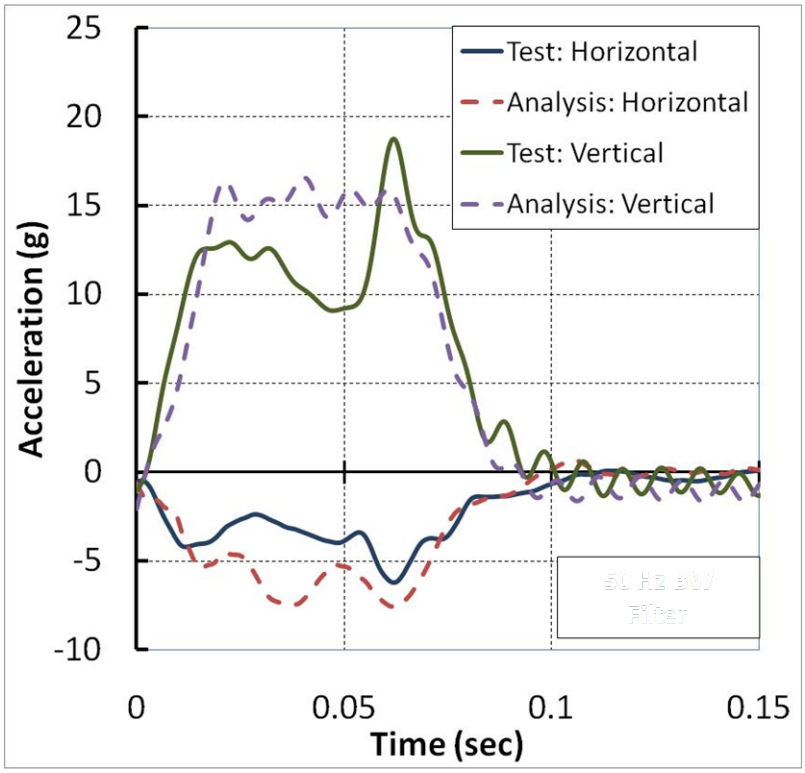


**Figure 9. Mass Simulator/DEA, Test versus Analysis Comparison, Acceleration**

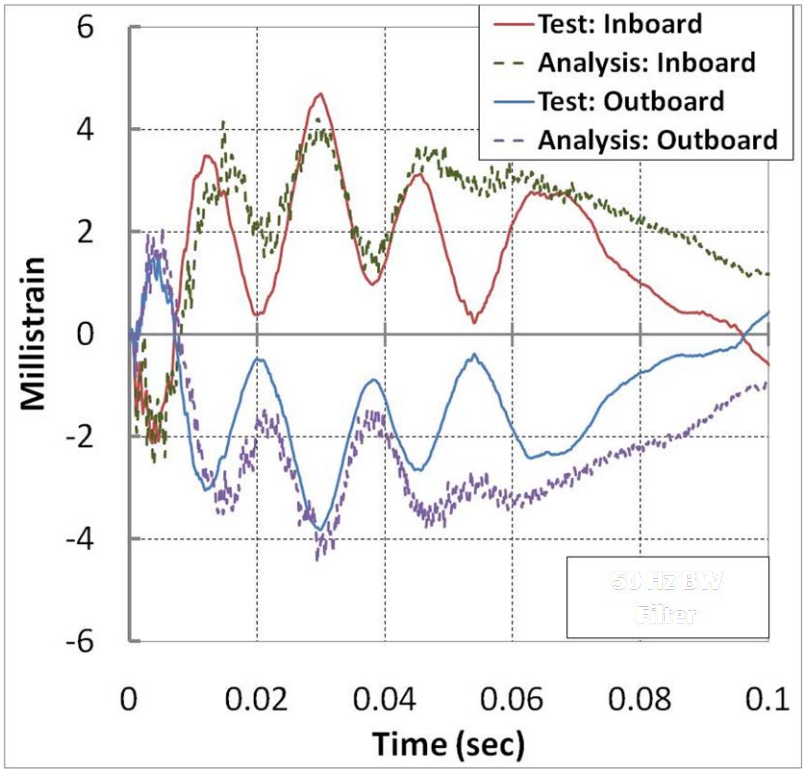


**Figure 10. Mass Simulator/DEA, Test versus Analysis Comparison, Strain**

A computer aided design (CAD) model of the MD-500 fuselage was provided by the Army Aviation Applied Technology Directorate (AATD) and imported into the finite element pre-processor Hypermesh [11]. The geometry models consisted of surface representations of the fuselage outer mold line (OML), bulkheads, seat pan, and floor. The additional ribs, keel beam, and stiffeners not present in the baseline geometry were based on hand measurements and augmented onto the existing geometries. Thickness measurements were taken using ultrasonic transducers and calipers. Material densities were scaled up to represent mass of additional ribs and stiffeners not discretely modeled.

The LS-DYNA FEM of the MD-500 fuselage is shown in Figure 11. The size of the fuselage model is 27,000 elements with much of the refinement concentrated around the subfloor. The fuselage model is composed of shell and mass elements. The lifting fixture, pullback fixture, and data acquisition system (DAS) platform were modeled as *MAT_020 rigid shells. Material properties for the fuselage are based on the MD-500 Structural Repair Manual [12] and include *MAT_003 Aluminum 2024-T3, *MAT_001 fiberglass, and *MAT_001 Kevlar fabric.

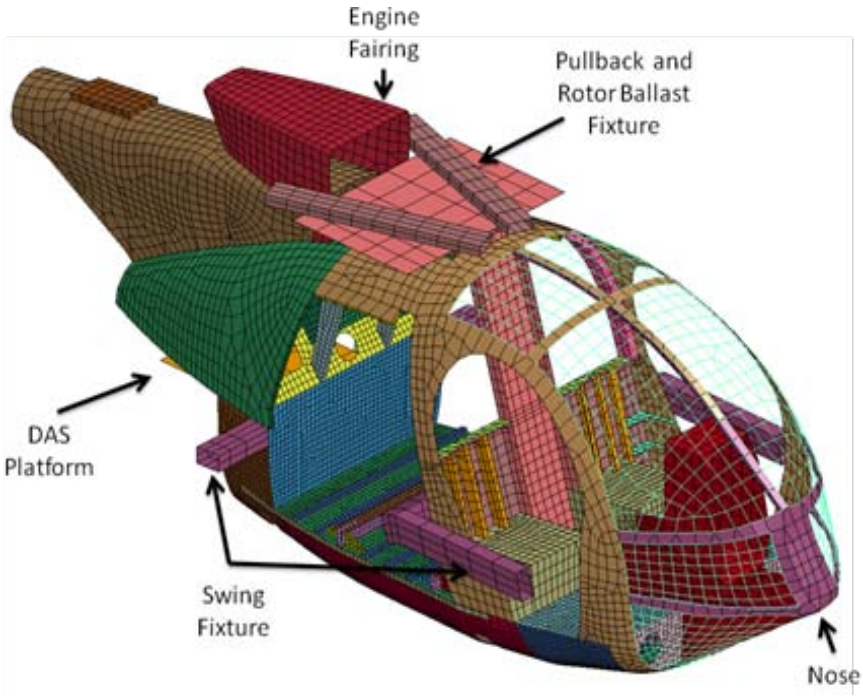


**Figure 11. MD-500 Fuselage FEM**

Crew seat and passenger bench seat geometries, containing aluminum frames and nylon mesh fabric stretched over the frames, were constructed. Targets were attached to the seat, and point clouds were generated and converted to parametric solids with 3-D photogrammetric techniques, as shown in Figure 12. The seat fabric material properties were determined by dynamic drop tests of a 20 lb hemispherical mass onto the fabric. The drop test was simulated with an FEM, and the modulus of the fabric was modified to match accelerations from the test. Figure 13 shows the drop test setup, FEM simulation, and acceleration data comparison. The effective dynamic modulus calculated is 4,000 psi. This modulus is almost three times higher than the modulus determined from quasi-static load cell testing.


**Figure 12. Seat FEM**

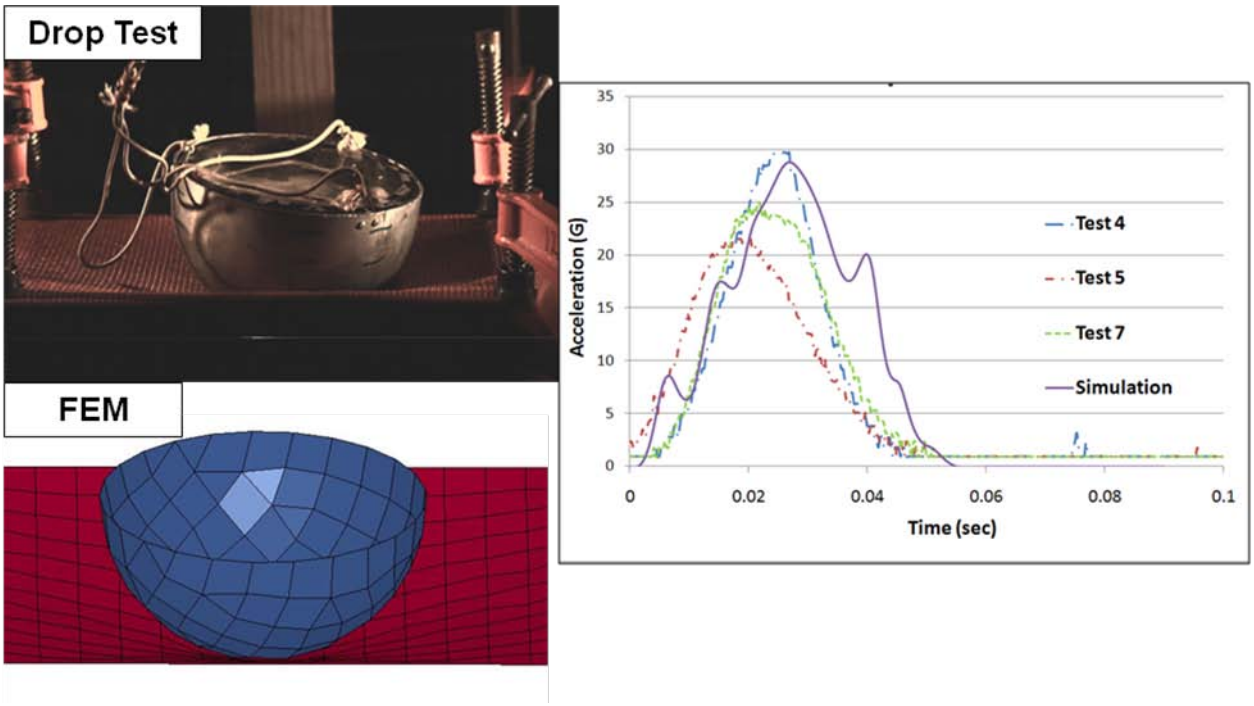


**Figure 13. Seat Mesh Dynamic Testing**

A model of the 50th percentile HYBRID III male, provided by LSTC, was used for the HYBRID II and III ATDs [13]. The biofidelic HSTM50, containing thoracic organs, skeletal structure, and soft tissue, is mated to a HYBRID III pelvis and legs and seated within the passenger

compartment [4]. A reduced human torso FEM was constructed and adapted from the Human Torso Finite Element Model (HTFEM) [14]. The organs and soft tissue elements are represented by solid silicone elements. The sternum, ribcage, vertebrae and scapula are modeled with fiberglass bar and shell elements. The bar and shell elements are embedded within the solid elements and coupled using *CONSTRAINED_LAGRANGE_IN_SOLID. The reduced human torso FEM was attached to the LSTC FEM pelvis and legs. The ATD FEM's are shown in Figure 14. The pilot and co-pilot ATDs are restrained with four point harnesses, and the passenger and HSTM50 are restrained with three point harnesses. Seatbelt shell elements were fitted to the torso and pelvis using the *BeltFit* option within LS-PREPOST.

The system integrated LS-DYNA FEM of the MD-500 is shown in Figure 15. The FEM has approximately 400,000 elements. The total weight of the test article and FEM is 2,930 lb.

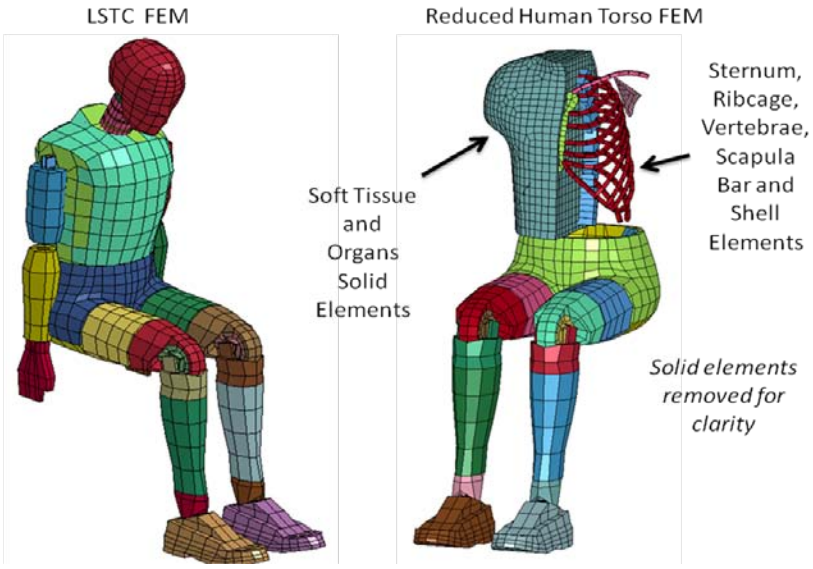


**Figure 14. ATD FEM's**

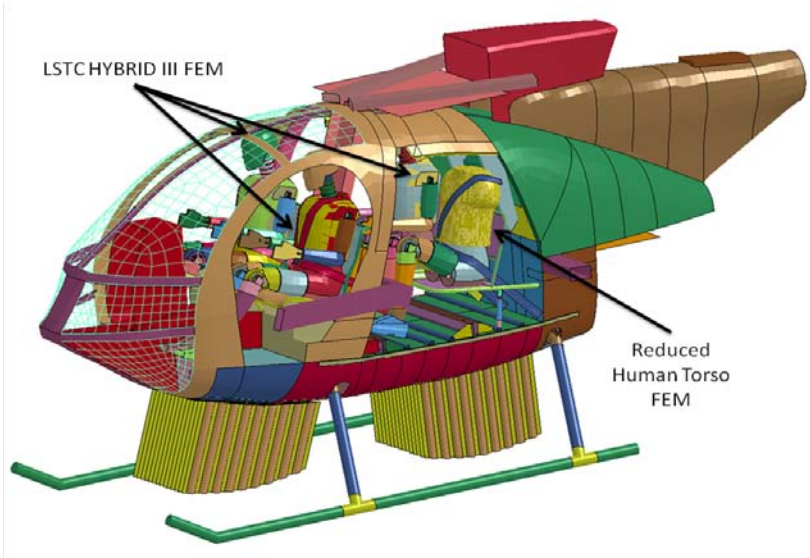


**Figure 15. MD-500 FEM**

## MD-500 Pre-Test Analysis

Pre-test simulations were conducted with the system integrated FEM to identify potential damaged regions and to predict occupant loads. Throughout the model development process, the mesh was locally refined and detail was added to the fuselage FEM to ensure all critical loads paths were captured. Modifications were made to the test article to limit damage and provide minimal reinforcement. A doubler composed of four layers of 0.010 in. thick graphite epoxy fabric was bonded to the belly skin. The orientation of the rear DEA was changed from 20 degrees to zero degrees to optimize the relative line of action between the DEA, the surface, and the belly.

There was concern that the compliance of the seat mesh would cause the pilot and co-pilot pelvises to impact the seat box, which is the airframe structure directly underneath the seat pan. To determine the effect of the seat mesh impacting the seat box, a foam wedge was placed underneath the co-pilot seat. The co-pilot seat would presumably track the seat box response more closely.

The average vertical accelerations at the semi-rigid swing fixture are shown in Figure 16 for simulations with and without the DEA. The height of the swing fixture is near the vertical CG position of the test article. With the DEA, the average load at the swing fixture is nearly 10 g with duration of roughly 90 milliseconds. The peak acceleration for the case without the DEA exceeds 30 g with duration of 60 milliseconds. The addition of the DEA reduces the peak load by about two-thirds.

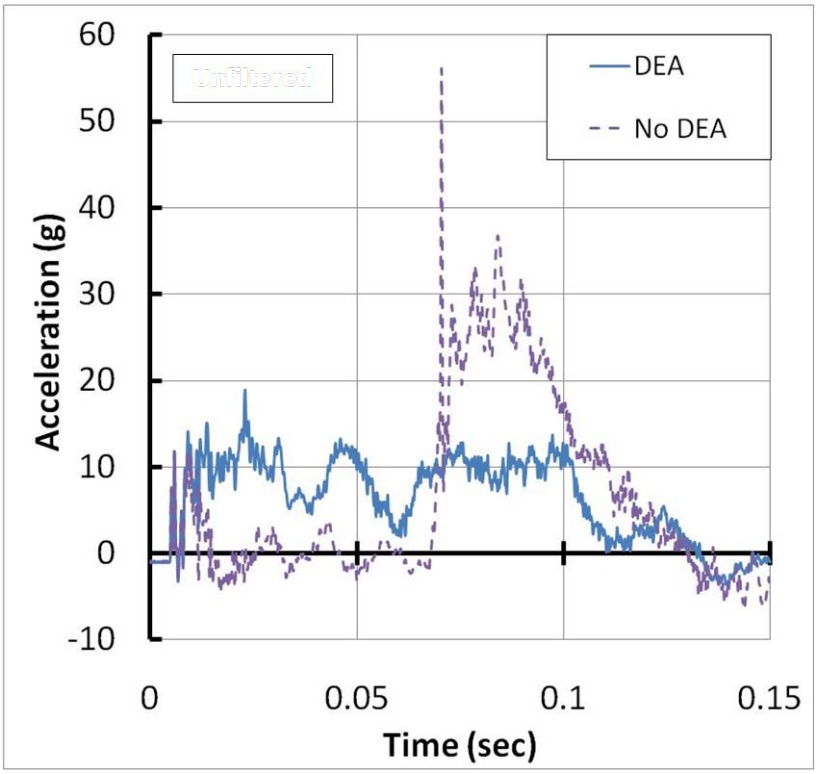


**Figure 16. Pre-Test, Vertical Acceleration, Swing Fixture**

The vertical pelvic accelerations are plotted for all four ATDs in Figure 17. The passenger and HSTM pelvic loads track the response of the swing fixture, with slightly higher magnitudes (15 g versus 10 g). The pilot and co-pilot loads are notably higher with 22 to 25 g initial peaks. There is a time delay between the pilot and co-pilot response as the co-pilot seat interacts with the foam wedge earlier than the pilot impacts the seat box, but the peak acceleration is not reduced by the presence of the foam wedge.

Based on the Aircraft Crash Survival Design Guide [15], the human tolerance level for loads directed along the spinal axis is 20-25 g. The pre-test predictions show that the occupant responses with the DEA are within this limit. An additional criteria associated with spinal injury is specified in FAR Part 27.562 [16]. The compression load threshold is 1,500 lb. The lumbar loads for the pilot, co-pilot, and passenger are plotted in Figure 18. The peak lumbar loads are 900 lb and well within the 1,500 lb allowable.

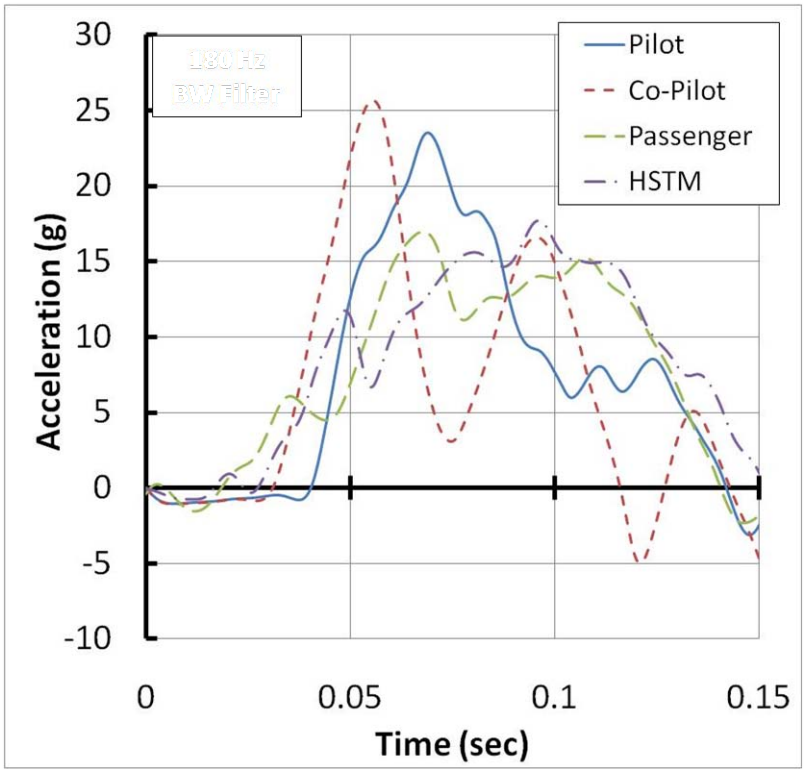


**Figure 17. Pre-Test, ATD Vertical Pelvic Accelerations**

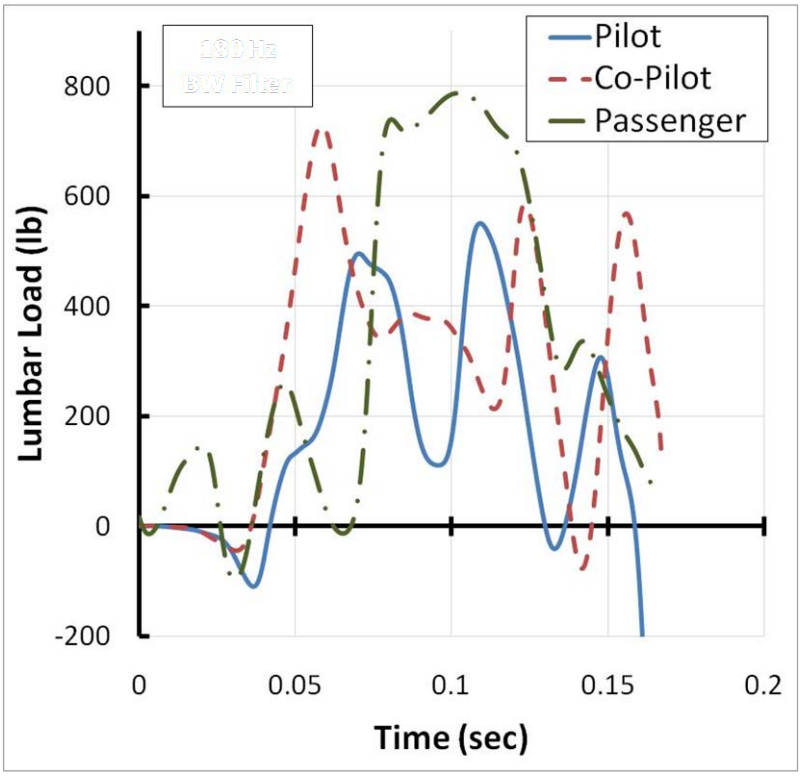


**Figure 18. Pre-Test, ATD Vertical Lumbar Loads**

## MD-500 Full Scale Test

The full-scale test was conducted in December 2009 at the LandIR facility at LaRC. The vehicle displacement time history was recorded using 2-D and 3-D photogrammetry. The test article impacted with 38.7 ft/sec horizontal and 25.5 ft/sec vertical velocity, and 5.7 degrees pitch, 9.3 degrees yaw, and 7 degrees roll. The off attitude impact conditions are attributed to a combination of factors including inconsistent swing cable preloads and longitudinal offset between the swing cable effective line of action and the CG.

Overall, the damage to the test article was minor. Impact occurred initially on the front right skid gear. Slight tears in the skin above the fuselage opening were evident for both skid gears. The DEA restraint support rail impeded the gear from additional movement with the result that the right gear bent along the rail. Damage along the fuselage belly was limited to the right front section of belly forward of the front bulkhead.

The MD-500 FEM was reoriented to the test impact conditions. Additionally, the crush tubes were redefined to include rotational stiffness not present in the pre-test simulations. The overall rotation of the struts is restricted by the rod end fittings and mating clevises. This locking effect is not seen in the zero pitch, roll and yaw cases where the DEA does not fully compact. For the test orientation, the DEA along the right side nearly bottoms out and the lack of strut rotational stiffness causes the fuselage to roll to the right side. This roll motion was not observed during the impact and slide out. A discrete beam (*SECTION_BEAM, ELFORM 6) was substituted for the truss element with an axial load versus deflection curve equivalent to the elastic/plastic curves and bending moment versus rotation curves that include a stop angle of 10 degrees.

## Test and Analysis Comparison

A detailed summary of the test responses is provided in [17]. The test impact orientation and deformation at peak load is shown for test and analysis in Figure 19. The global deformation pattern of the deployable energy absorber is similar to the deformation observed in the high speed video, primarily folding on the right side and crushing on the left side. However, upon further examination, the locations where the DEA folded and compacted and consequently transferred high impact loads locally do not correlate. The damage to the front right side did not occur in the analysis. Within the simulation, dimpling of the skin occurred in the region above the rear DEA, whereas the post-test inspection revealed no damage. The DEA folding, crushing and sliding along the belly was partially captured with the shell-based model. The addition of lateral loading within the DEA contributed to this behavior.

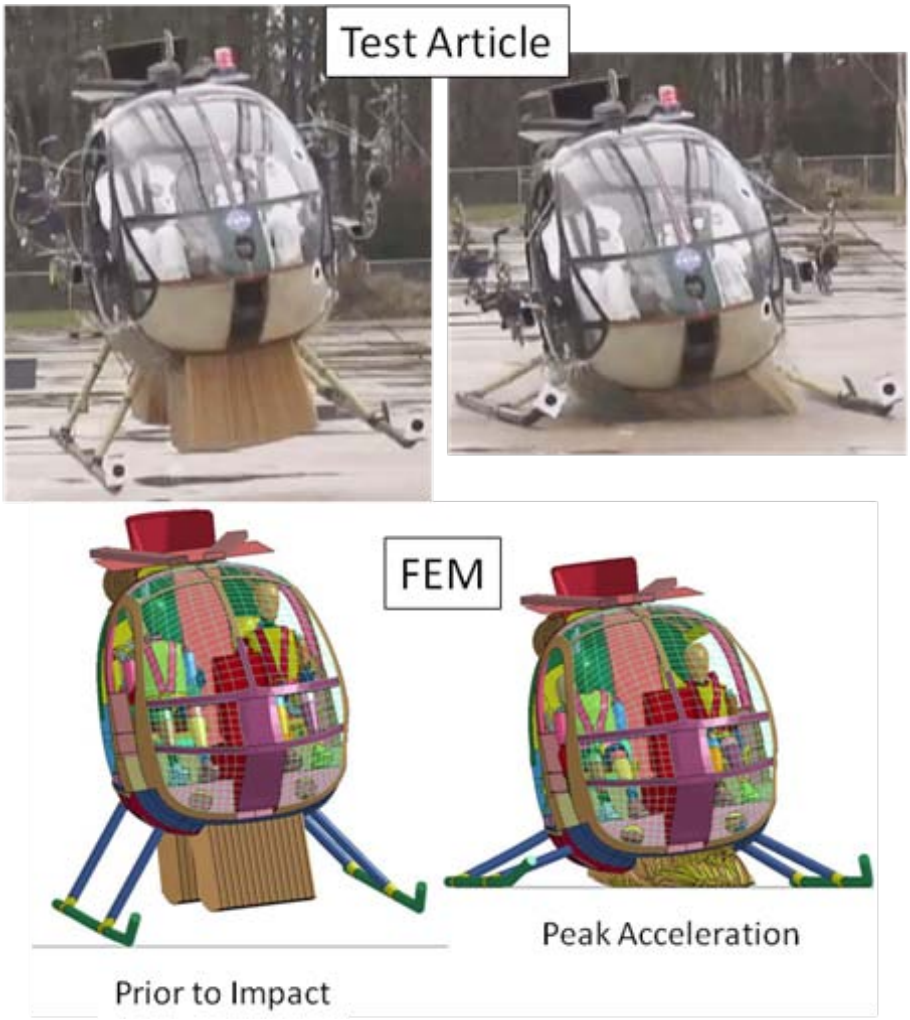


**Figure 19. MD-500 FEM Deformation**

The test acceleration pulse shapes are effectively trapezoidal with duration of roughly 0.12 seconds. The data comparisons are plotted for 0.2 seconds. All acceleration and force data are low-pass filtered with a Butterworth 180 Hz filter.

No accelerometers were positioned near the vehicle CG. Therefore, an overall global acceleration was derived from photogrammetric velocity output of a target located near the CG. This acceleration was plotted with the MATSUM vertical acceleration of the swing fixture in Figure 20. There is good agreement in terms of magnitude and impulse for the fuselage.

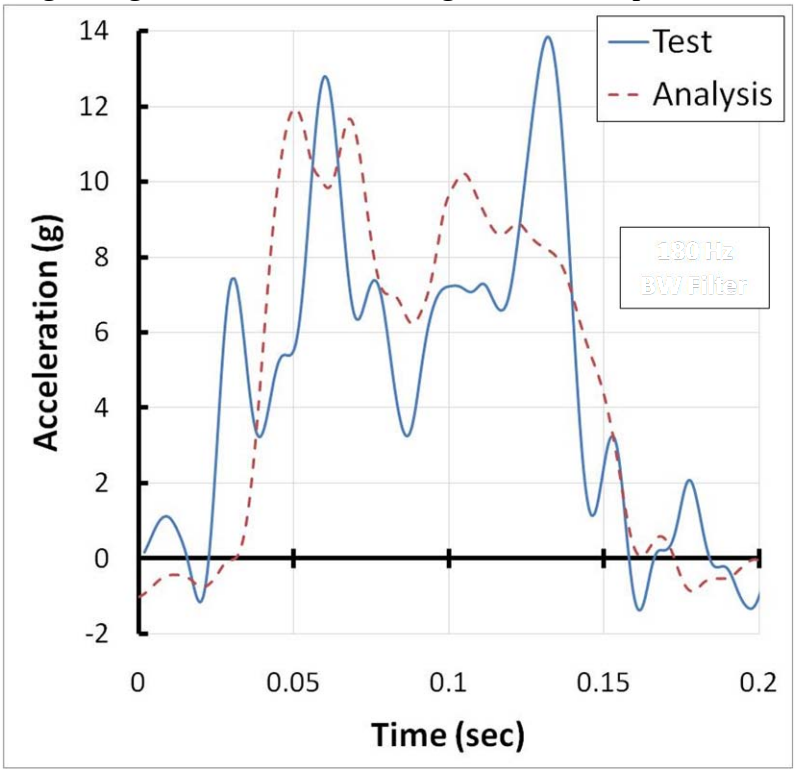


**Figure 20. Global Vertical Acceleration**

The nodal vertical acceleration on the pilot seat box is plotted against test data in Figure 21. The reference coordinate system for the simulation and the test are fixed along the floor surface. The axis perpendicular to the floor represents vertical. The measured and analysis accelerations are comparable with a single sharp peak present in the analysis. Figure 22 shows the comparison of pilot ATD vertical pelvic acceleration. The measured ATD pelvic acceleration is around 10 g and more uniformly spread than the analysis pelvic acceleration. This load is considered survivable and within the level of voluntary exposure [15]. The higher peak load seen in the analysis possibly indicates that the pilot dummy preload is not properly pre-tensioned against the seat mesh and spurious impact loads are imparted between the ATD and seat and seat box.

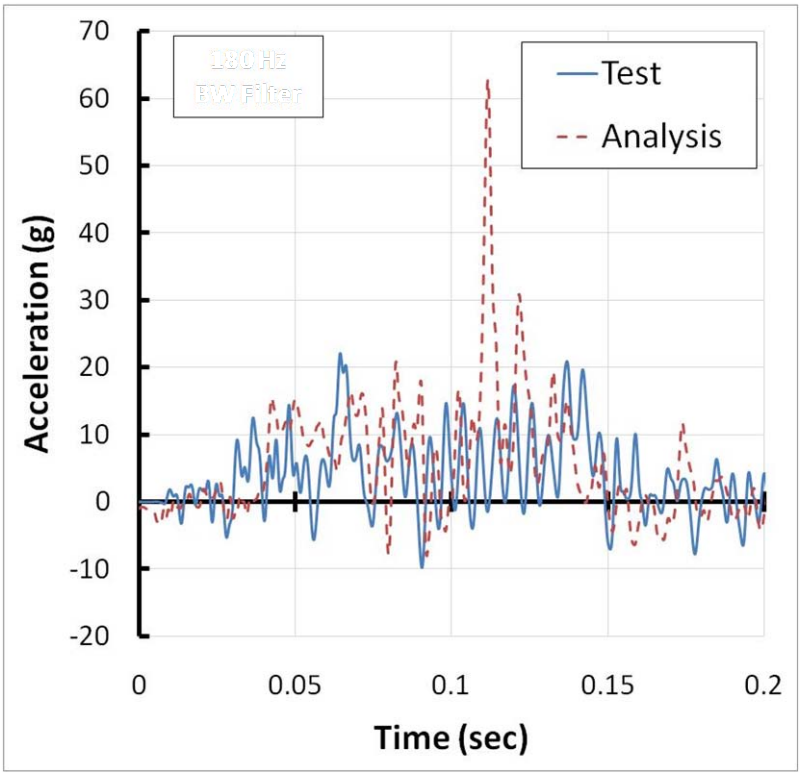


**Figure 21. Pilot Seat Box Vertical Acceleration**

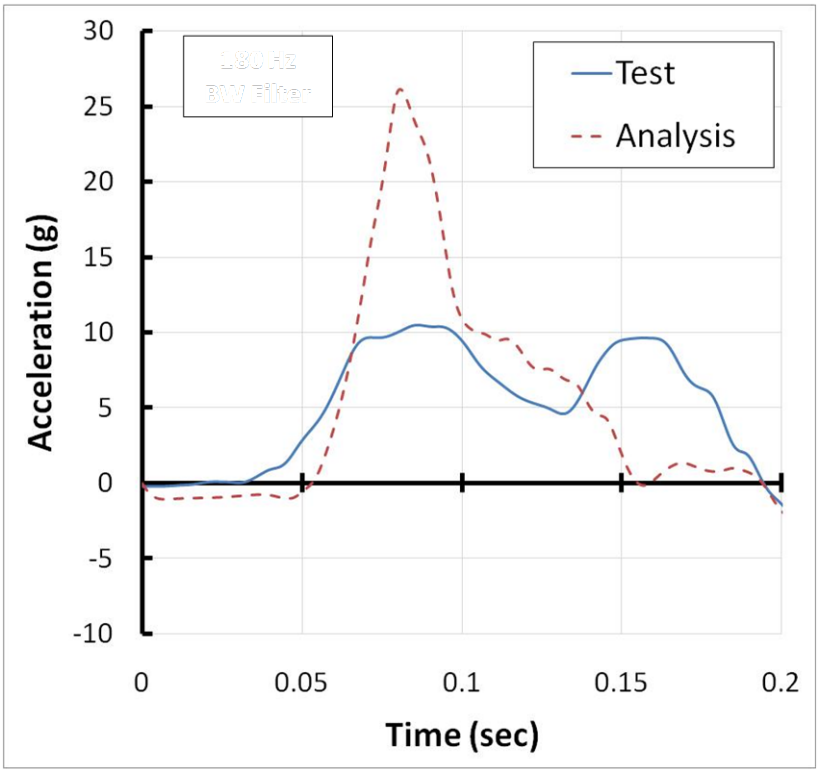


**Figure 22. Pilot Pelvic Vertical Acceleration**

The measured and analysis pilot lumbar loads are plotted in Figure 23. The test data indicated that the peak loads are well within the 1,500 lb injury criteria. The measured loads considerably

exceed the analysis loads and the overall responses differ. Also evident in Figure 22 and Figure 23, the measured pulse shapes for the lumbar loads and the pelvic accelerations are similar for the pilot. The lumbar loads could consequently be scaled from the pelvic accelerations. The pilot ATD FEM does not produce similar pulse shapes between lumbar load and pelvic acceleration.

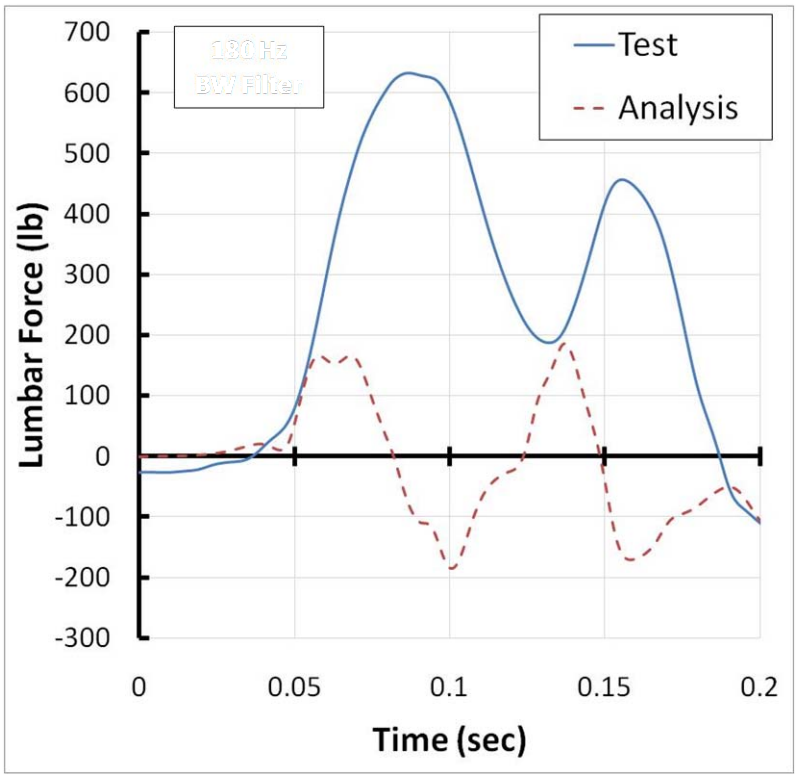


**Figure 23. Pilot Lumbar Loads**

The nodal vertical acceleration on the floor centerline beneath the passenger seats is plotted against test data in Figure 24. This location relates to the input to the passenger bench. The accelerations and pulse shapes compare well, with magnitudes between 12 and 17 g. The passenger pelvic accelerations and lumbar loads are shown in Figure 25 and Figure 26, respectively. The analysis responses have differing magnitudes and pulse shapes for both pelvic vertical acceleration and lumbar load when compared to test. In spite of the discrepancy between test and analysis responses, the passenger ATD FEM does produce similar pulse shapes relating lumbar load to pelvic acceleration.

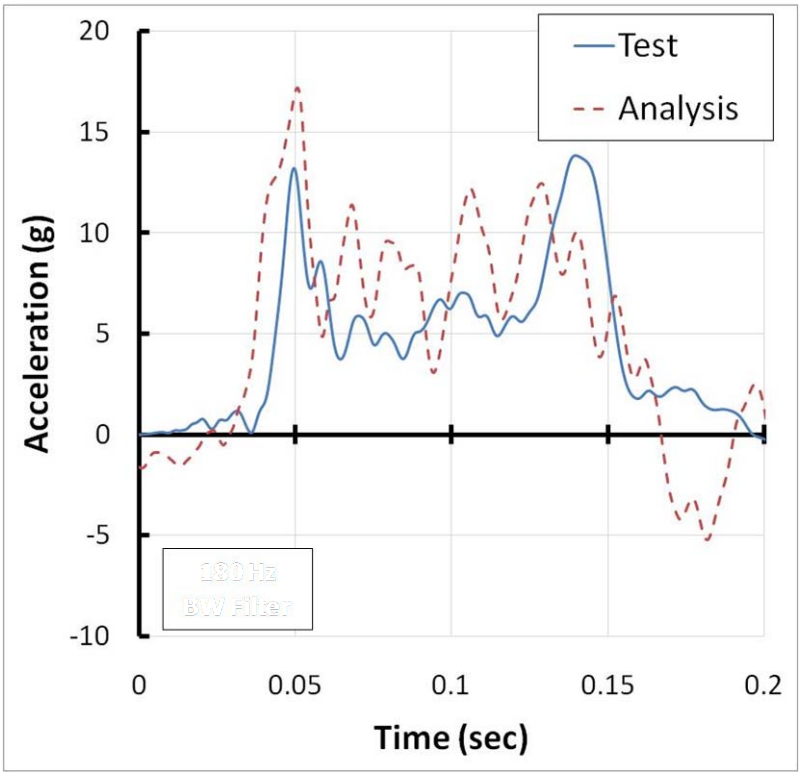


**Figure 24. Passenger Floor Vertical Acceleration**

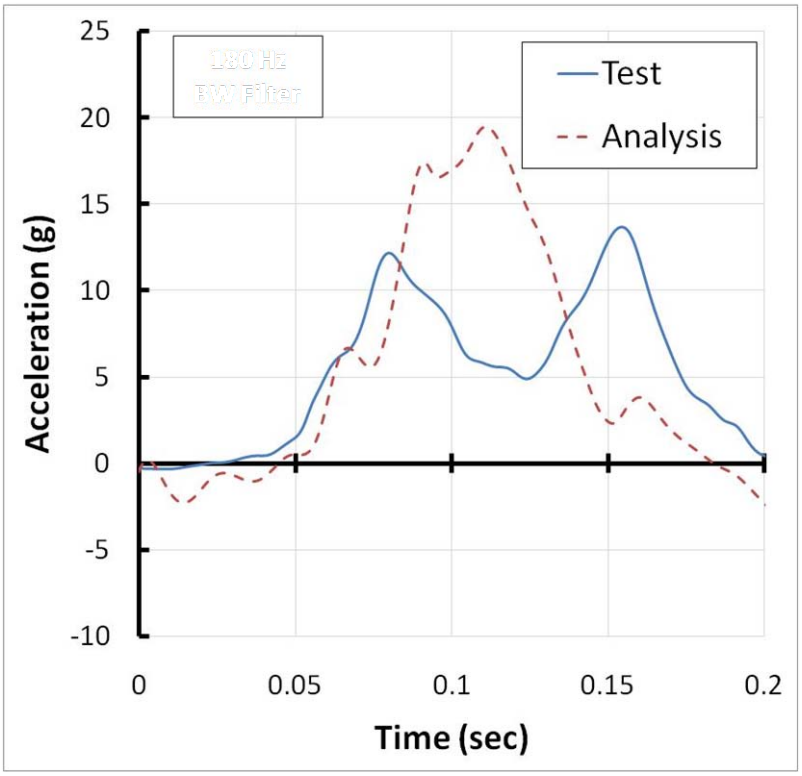


**Figure 25. Passenger Pelvic Vertical Acceleration**

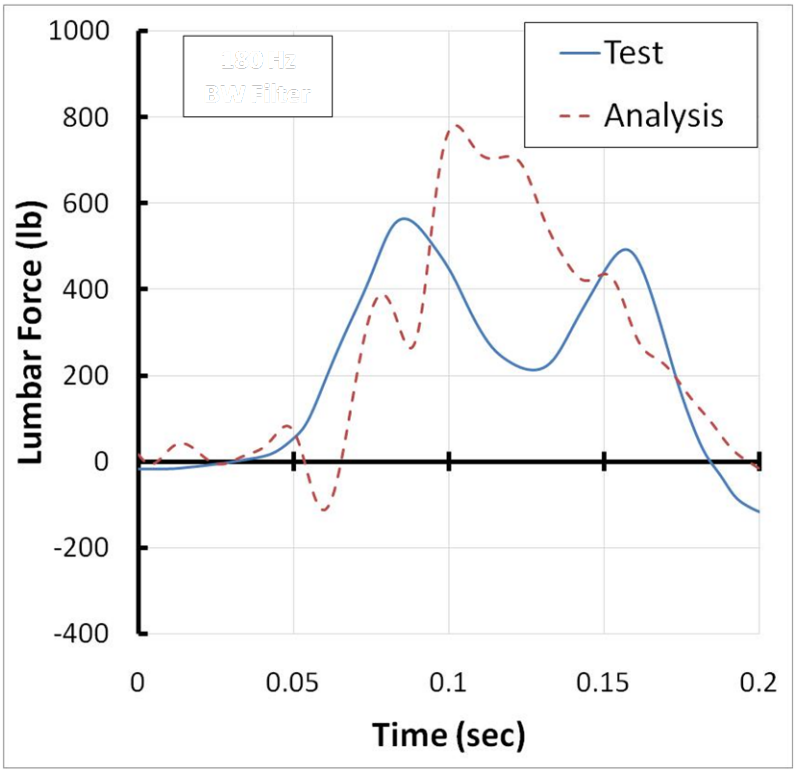


**Figure 26. Passenger Lumbar Load**

The inconsistencies in ATD responses may be due to the ATD models alone or the complex interaction between the ATD, seat, and restraint. The LSTC ATD models have been calibrated for frontal impacts conditions. Test and analysis correlation efforts for vertically loaded seated occupants are in their initial stages. Sled tests with the seat backs oriented parallel to the track were conducted by Tabiei *et al* [18]. Several ambiguities were discovered for acceleration and force data and analysis correlation was highly sensitive to dummy and restraint positioning. Further investigation is required to resolve these discrepancies.

## Conclusion

A system integrated FEM has been developed concurrently with a full scale crash test of an MD-500 helicopter. The fuselage model was adapted from baseline OML geometry and augmented to include the skid gear and seats. The model also contains a shell based version of the DEA, three 50th percentile HYBRID III male ATD FEM's provided by LSTC, and a fourth biofidelic torso/HYBRID III pelvis FEM.

Component level analyses and tests were conducted to establish the material properties of the DEA, the crush tubes, and the seat mesh. Full-scale mass simulator tests were conducted to develop confidence in both analysis and test methodologies and reduce risk. Good agreement for skid gear strains and CG accelerations was seen between test and analysis. A pre-test simulation revealed minimal damage to the fuselage, and occupant loads that were within the survivable injury limits.

Following the full-scale test, minor damage was observed to the skid gear and front right belly. The vehicle vertical accelerations were attenuated to peaks of 10-15 g, signifying excellent performance by the DEA's despite the off-nominal attitude at impact. The fuselage accelerations

matched well between test and analysis. There were discrepancies between test and analysis for occupant loads. These ATD FEM occupant models must be studied further for the vertical impact loading conditions considered here. The system integrated FEM has proven to be a valuable and effective predictive tool that can account for multiple crashworthy rotorcraft elements and their critical interactions.

## References


1. Jackson, K.E., Fuchs, Y., and Kellas, S., "Overview of the NASA Subsonic Rotary Wing Aeronautics Research Program in Rotorcraft Crashworthiness," Journal of Aerospace Engineering, Special Issue on Ballistic Impact and Crashworthiness of Aerospace Structures, Volume 22, No. 3, July 2009, pp. 229-239.
2. Khalil, T.B. and Sheh, M.Y., "Vehicle Crashworthiness and Occupant Protection in Frontal Impact by FE Analysis – An Integrated Approach", Proceedings of Crashworthiness of Transportation Systems: Impact and Occupant Protection, Kluwer Academic Publisher, pp. 363-399, 1997.
3. Kan, C.D., Marzougui, D., Bahouth, G. T., and Bedewi, N. E., "Crashworthiness Evaluation using Integrated Vehicle and Occupant Finite Element Models," International Journal of Crashworthiness. Vol. 6, no. 3, pp. 387-397. 2001
4. Roberts, J., Merkle, A., Biermann, P., Ward, E., Carkhuff, B., Cain, R., and O'Connor, J., "Computational and Experimental Models of the Human Torso for Non-Penetrating Ballistic Impact", J. Biomech., 40 (1), 2007, pp. 125-136.
5. Kellas, S., "Deployable Rigid System for Crash Energy Management," US Patents 6,755,453, June 29, 2004, 6,976,729 December 20, 2005, and 7,040,658 May 9, 2006.
6. Kellas, S., and Jackson, K.E., "Deployable System for Crash-Load Attenuation," Proceedings of the 63rd AHS Annual Forum, Virginia Beach, VA, May 1-3, 2007.
7. Kellas S. and Jackson K.E., "Multi-Terrain Vertical Drop Tests of a Composite Fuselage Section," Proceedings of the 64th AHS Annual Forum, Montreal, Canada, April 29, May 1, 2008.
8. Kellas, S., Jackson, K., and Littell, J., "Full Scale Crash Test of a MD 500 Helicopter with Deployable Energy Absorbers," Proceedings of the 66th AHS Annual Forum, Phoenix, AZ, May 11-13, 2009.
9. Polanco, M., "A Parametric Study on a Shell-Based Model of a Kevlar/Epoxy Composite Honeycomb," AHS Technical Specialists Meeting on Rotorcraft Structures and Survivability, Williamsburg, VA, October 27-29, 2009
10. Jackson, K. E., A Parametric Study on a Solid-Based Model of a Kevlar/Epoxy Composite Honeycomb," AHS Technical Specialists Meeting on Rotorcraft Structures and Survivability, Williamsburg, VA, October 27-29, 2009
11. Anon, Hypermesh, Version 9.0, Altair Inc., Troy, MI.
12. Anon, Structural Repair Manual, CSP–SRM–6, MD Helicopters, Inc, Mesa, AZ, May 2006.
13. Guha, S., Bhalsod, D., and Krebs, J., "LSTC Hybrid III Dummies, Positioning & Post-Processing, Dummy Version: LSTC.H3.103008_v1.0," LSTC Michigan, October 30, 2008
14. Roberts, J., Merkle, A., Biermann, P., Ward, E., Carkhuff, B., and O'Connor, J., "Modeling the Human Torso to Study BABT," Journal of Biomechanics, Volume 40, Supplement 2, August 2007, S47.
15. Desjardins, S., Laananen, D., Singley, G., "III: Aircraft Crash Survival Design Guide," USARTL-TR-79-22A, Applied Technology Laboratory, US Army Research and Technology Laboratories, Ft. Eustis, VA, 1979.
16. Code of Federal Regulations, Federal Aviation Regulations for Aviation Maintenance Technicians FAR AMT, Part 27 Airworthiness Standard: Normal Category Rotorcraft, 27.562 Emergency Landing Dynamics.
17. Kellas, S., Jackson, K., and Littell, J., "Full Scale Crash Test of a MD 500 Helicopter with Deployable Energy Absorbers," Proceedings of the 66th AHS Annual Forum, Phoenix, AZ, May 11-13, 2009.
18. Tabiei, A., Lawrence, C., and Fasanella, E., "Validation of Finite Element Crash Test Dummy Models for Predicting Orion Crew Member Injuries During a Simulated Vehicle Landing," NASA/TM—2009-215476, March 2009.